OPEN

PRS GLOBAL OPEN EXPERIMENTAL

Structural and Mechanical Comparison of Human Ear, Alar, and Septal Cartilage

Ernst Jan Bos*†‡
Mieke Pluemeekers‡
Marco Helder†§
Nikolay Kuzmin¶
Koen van der Laan‖
Marie-Louise Groot¶
Gerjo van Osch‡**
Paul van Zuijlen*†††

Background: In the human ear and nose, cartilage plays a key role in establishing its form and function. Interestingly, there is a noticeable paucity on biochemical, structural, and mechanical studies focused on facial cartilage. Such studies are needed to provide elementary knowledge that is fundamental to tissue engineering of cartilage. Therefore, in this study, a comparison is made of the biochemical, structural, and mechanical differences between ear, ala nasi, and septum on the extracellular matrix (ECM) level.

Methods: Cartilage samples were harvested from 10 cadaveric donors. Each sample was indented 10 times with a nanoindenter to determine the effective Young's modulus. Structural information of the cartilage was obtained by multiple-photon laser scanning microscopy capable of revealing matrix components at subcellular resolution. Biochemistry was performed to measure glycosaminoglycan (GAG), DNA, elastin, and collagen content.

Results: Significant differences were seen in stiffness between ear and septal cartilage ($P = 0.011$) and between ala nasi and septal cartilage ($P = 0.005$). Elastin content was significantly higher in ear cartilage. Per cartilage subtype, effective Young's modulus was not significantly correlated with cell density, GAG, or collagen content. However, in septal cartilage, low elastin content was associated with higher stiffness. Laser microscopy showed a distinct difference between ear cartilage and cartilage of nasal origin.

Conclusion: Proposed methods to investigate cartilage on the ECM level provided good results. Significant differences were seen not only between ear and nasal cartilage but also between the ala nasi and septal cartilage. Albeit its structural similarity to septal cartilage, the ala nasi has a matrix stiffness comparable to ear cartilage.
(Plast Reconstr Surg Glob Open 2018;6:e1610; doi: 10.1097/GOX.0000000000001610; Published online 18 January 2018.)

*From the *Department of Plastic, Reconstructive and Hand Surgery, VU Medical Center, Amsterdam, The Netherlands; †CTRM/MOVE Research Institute, Amsterdam, The Netherlands; ‡Department of Otorhinolaryngology, Head and Neck Surgery, Erasmus University Medical Center, Rotterdam, The Netherlands; §Department of Orthopedic Surgery, VU Medical Center, Amsterdam, The Netherlands; ¶LaserLab Amsterdam, Department of Physics, Free University, Amsterdam, The Netherlands; ‖Department of Physics and LaserLab, Free University, Amsterdam, The Netherlands; **Department of Orthopaedics, Erasmus University Medical Center, Rotterdam, The Netherlands; and ††Red Cross Hospital Beverwijk, Beverwijk, The Netherlands.*

Received for publication May 21, 2017; accepted October 25, 2017.

DOI: 10.1097/GOX.0000000000001610

INTRODUCTION

Cartilage plays a key role with respect to form and function of facial features. When cartilage of the nose or ear is damaged by injury, it does not have the capacity to regenerate. This means that an ear or nose remains mutilated once its cartilage structure is disrupted. A reconstructive procedure is then necessary to create a new framework with a good 3D structure capable of withstanding normal mechanical forces. Practically, the reconstruction of the ala nasi or minor ear defects is most often performed using auricular or septal cartilage grafts.[1,2] In more extensive cases, costal

Disclosure: *The research by Mieke Pluemeekers was financially supported by SenterNovem in the framework of EuroNanoMed (EAREG-406340-131009/1). The research of Ernst Jan Bos was supported by the Dutch Burns Foundation. Neither of the other authors has any financial disclosures. The Article Processing Charge was paid for by the authors.*

Supplemental digital content is available for this article. Clickable URL citations appear in the text.

cartilage can be used, offering more material for harvest and providing a more rigid support. Ear, septal, or costal cartilage can be used for reconstruction, but the availability of material for transplantation is generally limited and donor-site morbidity remains a risk. This is especially the case in burn patients who often suffer from extensive damage to the nose and ears because of their protruded position and thin skin coverage.[1,3,4] As such, regenerative medicine offers exciting possibilities to overcome these problems. New developments in the field of tissue engineering have already found their way to the clinic. Yanaga et al., for example, performed several clinical experiments in which newly developed cartilage from autologous chondrocytes isolated from the ear was used for ear framework reconstruction.[2,5] With increased attention for tissue-engineered alternatives, we need structural information on the tissues we are seeking to replicate. However, there are little data in the literature on the mechanical characteristics and differences in composition and structure between the various facial cartilage types, in particular the ear, alar, and septal cartilage.

Although they share a common embryonic origin, facial cartilage soon differentiates into distinct cartilage subtypes according to their specific structural function. In the early stage of developing vertebrates, the embryonic region that is to become the head and neck is transiently divided into segments known as the pharyngeal arcs (PAs). The ear has a combined origin and is derived from PA1 and PA2 that form the hillocks of His at 6-week development. Eventually, these 6 hillocks fuse together to form the outer ear.[6,7] PA1 grows further outward to form the lower mandibular process and upper maxillary process. The latter later forms the frontal prominence and the medial and lateral nasal processes, which will form into the alar nasi and after final fusion into the septum.[8]

Mature ear cartilage consists of an intricate network of elastin fibers and collagen bundles surrounded by a layer of perichondrium. This high-elastin content makes it unique among the various cartilage subtypes in the facial region. The anatomy of the human nose on the other hand consists of several separate structural elements. A major part is the septum providing support for the bridge of the nose and on either side of the septolateral and lobular cartilages to support the ala nasi. The lateral area further comprises of several sesamoid cartilages and accessory cartilages. In contrast with ear cartilage, the nasal structures are all made of hyaline cartilage. Hyaline cartilage consists mainly of collagen, in particular type II, and is divided into several zones.[9]

The extracellular matrix (ECM) structure and its biochemical composition are essential to the mechanical function of cartilage. Standard biochemistry assays can be used to determine the concentration of the main tissue components. To visualize the 3D structure of the ECM, multiple-photon laser scanning microscopy has been used for other tissues such as articular cartilage.[10] This method is capable of revealing essential matrix components, ie, chondrocytes, collagen, and elastin fibers, label-free, with subcellular resolution and deep penetration.[11]

The reported stiffness of facial cartilage types varies considerably. Because different techniques are used to measure the cartilage, it is difficult to give a general value. Besides tensile or indentation measurements having different limitations and advantages,[12] it is also important to discern the different magnitudes or scale of mechanical testing. For the assessment of gross mechanical traits, important for maintaining of large shapes especially in surgical reconstruction, various techniques have been described.[13–16] The same applies for atomic force microscopy (AFM), where extensive research has been conducted on surface micro mechanics of cartilage.[17–19] However, the mechanical conditions of the scaffold's cellular environment, between AFM and gross mechanical testing, have important influence on the behavior of cells[20] and as such are fundamental to adequate regeneration of cartilage.[21] Therefore, insight in the local mechanical properties and structure on the ECM level is required to provide the right environment for cell differentiation. The device used in this study allows indentation on the micrometer scale at higher depth ranges, providing essential mechanical information on the different cartilage subtypes.

Understanding the fundamentals of tissue structures is essential for adequate tissue engineering. From practice, surgeons are familiarized with the gross mechanical traits of cartilage in reconstructive surgery. Mechanical behavior however is essentially determined on the microscopic scale through an intricate symbiosis of cells and their surrounding structures.

In this article, we aim to provide fundamental information on the differences between the facial cartilage types on a structural and mechanical level with the use of novel technology to evaluate these parameters on the ECM level. Although without direct practical implications, it may also offer surgeons new insights and inspiration in optimizing their reconstructive efforts by providing better understanding on the nature of the tissues they work with. With the advancement of regenerative medicine, surgeons will come to a point where this knowledge will prove invaluable.

METHODS

Samples

Cartilage samples were harvested from 10 fresh frozen cadaveric donors (8 male, 2 female), average age 66.5 ± 6 years at UMCU (University Medical Center of Utrecht, The Netherlands) according to the ethical guidelines of the institution. From each donor, 2 adjacent samples from the ear concha, medial nasoseptal cartilage, and lateral alar cartilage were removed with a 4-mm biopsy puncher. The samples were shipped at −20°C to either the VU University (Amsterdam, The Netherlands) for biomechanical and microscopic evaluation or EMC (Rotterdam, The Netherlands) for biochemical evaluation. Samples were thawed before experiments, and remaining tissue and perichondrium were surgically removed.

Indentation

To determine mechanical properties, indentation measurements were performed using a novel commer-

cial nanoindenter (Piuma; Optics11, Amsterdam, The Netherlands). The device utilizes a ferrule-top cantilever probe[22] to apply load and simultaneously measure indentation depth using a fiber optic–based readout (Figs. 1A, C). In this setup, a 78-µm diameter spherical probe was used capable of applying forces ranging from 0.1 µN to 7.5 mN at indentation depths ranging 1 to 17 µm. Cantilever bending calibrations were performed before each series of experiments by indenting a rigid surface and equating cantilever bending to probe displacement. Each sample was indented 10 times on the same anatomical location in a grid pattern with 100-µm distance between measurements. The resulting stress strain curves (Fig. 1B) were analyzed using the mathematic model derived by Oliver and Pharr for a spherical indenter to determine the effective Young's modulus (E*).[23] The indentation protocol was carefully optimized to minimize viscoelastic effects from influencing the measurements (data not shown).

Biochemical Evaluation

Before biochemical analysis, wet weight was determined of all cartilage samples, which were then digested overnight at 60°C in a papain solution (0.2M $Na_2H_2PO_4$, 0.01M EDTA.$2H_2O$, 250 µg/mL papain, 5 mM L-cysteine, pH 6.0).

The amount of DNA measured in each papain-digested cartilage sample was determined by ethidium bromide (GibcoBR1), using calf thymus DNA (Sigma-Aldrich) as a standard. Samples were analyzed with a spectrofluorometer (Wallac 1420 Victor 2; Perkin-Elmer, Wellesley, Mass.), using an extinction filter (340 nm) and an emission filter (590 nm).

A 1,9-dimethylmethylene blue (DMMB; pH 3.0) assay was performed to measure the sulfated glycosaminoglycan (GAG) content in each papain-digested cartilage sample. The metachromatic reaction of DMMB was monitored using a VersaMax spectrophotometer at 530 and 590 nm. Shark chondroitin sulfate C was used as a standard. Hydroxyproline content was measured to estimate collagen quantity using the Total Collagen Assay (QuickZyme Biosciences, Leiden, The Netherlands) according to the manufacturer's instructions. Briefly, papain digests were hydrolyzed with equal volumes of 12M HCl at 95°C for 18–20 hours. Hydroxyproline content was measured using a modification of the Prockop and Udenfriend method (Prockop and Udenfriend, 1960) and normalized to sample wet mass.

Elastin content of the cartilage samples was measured using the Fastin Elastin Assay (Biocolor, Carrickfergus, UK) according to manufacturer's instructions. Briefly, cartilage samples were converted to water-soluble α-elastin by 3 overnight heat extraction cycles at 100°C in 0.25M oxalic acid before adding the kit's dye. Absorption was measured at 513 nm on a VersaMax plate reader. α-elastin from bovine neck ligament (provided by manufacturer) was used as a standard.

Multiphoton Microscopy

Structural information of the cartilage was obtained by multiple-photon laser scanning microscopy using intrinsic optical signals from unprocessed cartilage. The imaging setup consisted of a commercial 2-photon laser scanning microscope (2PLSM, TriMScope I; Lavision BioTec GmbH)

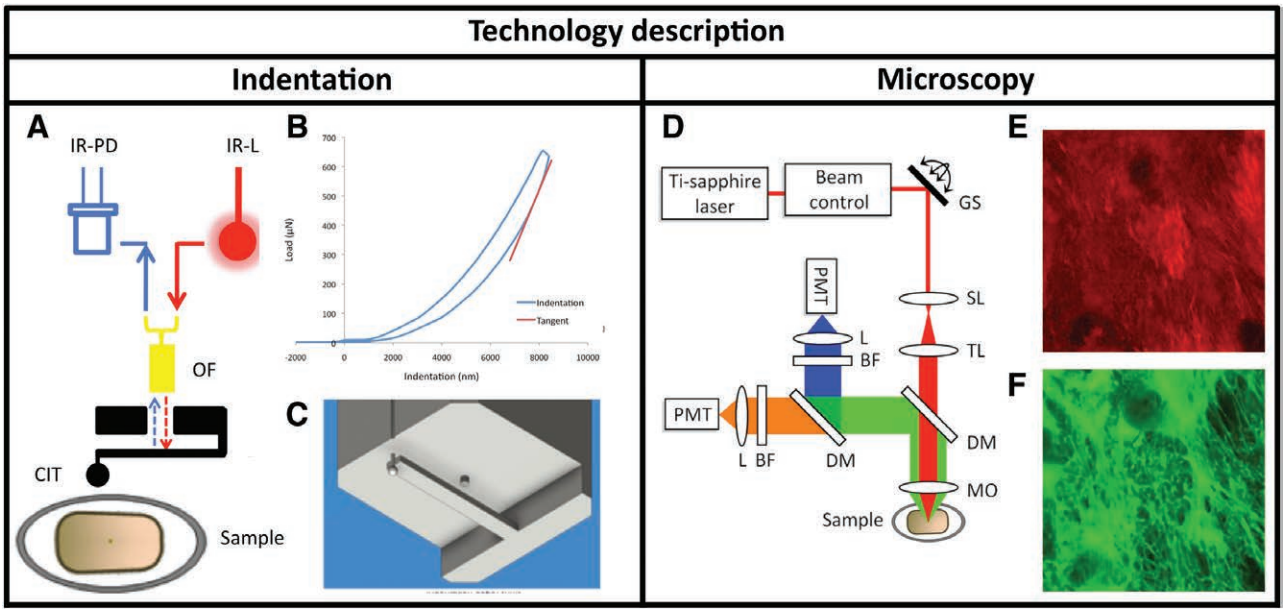

Fig. 1. Overview of indentation and multiphoton laser microscopy technology. A, Setup of cantilever indentation device (Piuma, Optics11). B, Example of indentation curve of a cartilage measurement. Red tangent represents the slope of the unloading curve used to determine the eff. Young's modulus. C, Graphic detail of the indenter tip, the ball forms the tip of the indenter (ϕ78 µm). D, Optical setup of multiphoton laser scanning microscope TriMScope I (LaVision Biotech), titanium-sapphire laser. E, SHG channel showing collagen bundles. F, 2PF channel showing elastin fibers. BP, band-pass filters; CIT, cantilever indentation tip; DM, dichroic mirror; GS, X-Y galvo scanner mirrors; IR-L, infrared laser; IR-PD, infrared laser diode; L, lenses in the front of the PMTs; MO, microscope objective; OF, optical fiber; PMT, photomultiplier tubes; SL, scan lens; TL, tube lens.

and a femtosecond laser source (Fig. 1D). The laser source was a femtosecond Ti-sapphire laser (Coherent Chameleon Ultra II) generating ~200 fs pulses at 800 nm with linear polarization and repetition rate of 80 MHz. The laser beam was focused on the cartilage sample by a 25×1.10 large N.A. water-dipping objective (Nikon APO LWD), providing transverse resolution ~0.5 µm and axial resolution of ~2 µm. The laser power on the sample was adjusted in the range 5–50 mW to attain sufficient signal-to-noise ratio and avoid tissue photodamage. The laser beam was transversely scanned over the sample by a pair of galvo mirrors. Depth scanning was accomplished by moving the objective with a stepper motor.

The second harmonic (SHG) and 2-photon fluorescence (2PF) photons were generated by collagen (SHG, 2PF) and elastin (2PF) fibers and by intracellular autofluorescent proteins and were collected in the epidetection geometry. The SHG and 2PF photons were filtered from the 800-nm excitation photons by a dichroic mirror (Chroma T695lpxrxt), then split into SHG and 2PF channels by a dichroic mirror (Chroma 425lp), passed through interference filters for SHG (Chroma Z400/10X) and 2PF (Chroma HQ500/140M-2P), and detected by high-sensitivity GaAsP photomultiplier tubes (Hamamatsu H7422-40) (Figs. 1E, F).

Data acquisition was performed with the TriMScope I software ("Imspector Pro") and images stacks were stored in 16-bit tiff format and further processed and analyzed with "ImageJ" software (MacBioPhotonics).

Statistical Analysis

Biochemical differences were analyzed using mixed models with Bonferroni correction. Differences in effective Young's modulus between groups were determined through generalized estimating equations. To measure the correlation between stiffness and biochemical content, a bivariate correlations model was used. All analyses were performed using SPSS Statistics software version 22. A P value of less than 0.05 was considered significant.

RESULTS

Indentation

Indentation revealed significant differences ($P = 0.011$) in stiffness between ear cartilage (1.14±0.71 MPa) and septal cartilage (2.65±1.78 MPa) and between ala nasi cartilage (1.26±0.51 MPa) and septal cartilage ($P = 0.005$) (Fig. 2). Comparison of ala nasi with ear cartilage showed no significant differences however. The stiffness per cartilage type varied considerably between donors (**see Figure, Supplemental Digital Content 1**, which displays stiffness varied considerably between donors per cartilage type, ***http://links.lww.com/PRSGO/A624***).

Biochemistry

Cell density based on DNA content was significantly higher in ala nasi cartilage (2.35±1.20 µg/mg dry weight) than in cartilage from the ear (1.13±0.23 µg/mg dry weight) or septum (0.94±0.52 µg/mg dry weight) ($P = 0.005$ and $P = 0.001$, respectively) (Fig. 3A). Auricular cartilage (141.40±27.2 µg/mg dry weight) had a significantly higher elastin content than ala nasi (60.12±18.35 µg/mg dry weight) and septum (17.38±16.71 µg/mg dry weight) (Fig. 3B). Water and collagen content were not significantly different between the cartilage types (Fig. 3C). In the nose, septum (96.00±23.21 µg/mg dry weight) appeared to have slightly higher GAG content than ala nasi (64.61±30.42 µg/mg dry weight) (Fig. 3D).

Per cartilage subtype, the effective Young's modulus was not significantly correlated with cell density, GAG, or collagen content. However, in septal cartilage, low elastin content was associated with higher stiffness (Table 1).

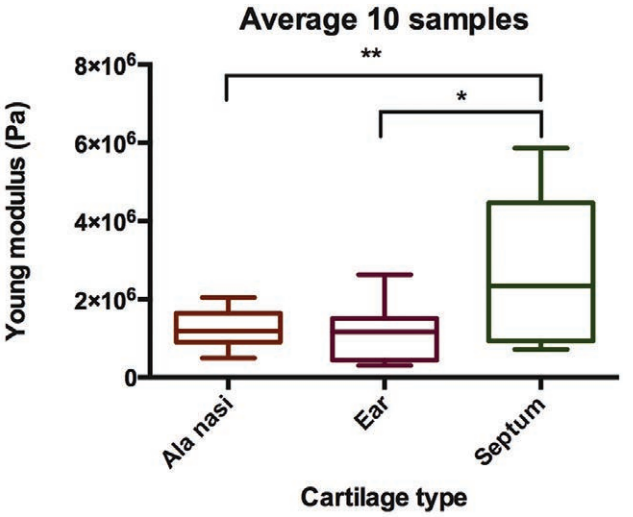

Fig. 2. Indentation revealed significant differences in stiffness between ear cartilage and septal cartilage (*P = 0.011) and between ala nasi cartilage and septal cartilage (**P = 0.005). No significant differences between ala nasi and ear cartilage were seen.

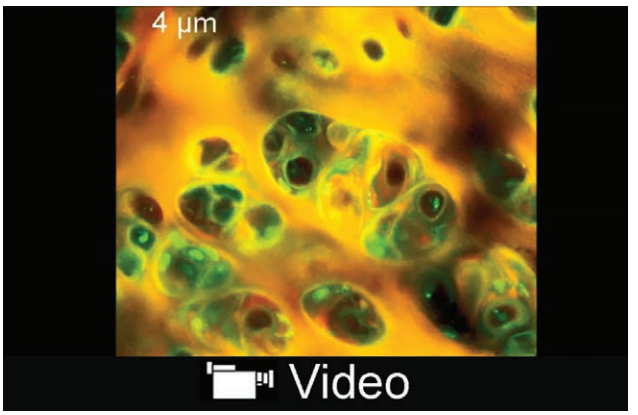

Video Graphic 1. See video, Supplemental Digital Content 2, which displays multiple-photon laser scanning microscopy of the architecture of the ala nasi cartilage in 3D stacked image video. Unlike the ear cartilage, no elastin is seen other than a diffuse green background signal. The majority of cells are grouped in relatively large clusters. Step size, 2 µm; green, elastin; red, collagen, ***http://links.lww.com/PRSGO/A625***.

Multiphoton Microscopy

The cartilage samples of 2 donors were imaged in the mid segment in the sagittal plane. The SHG and 2PF mi-

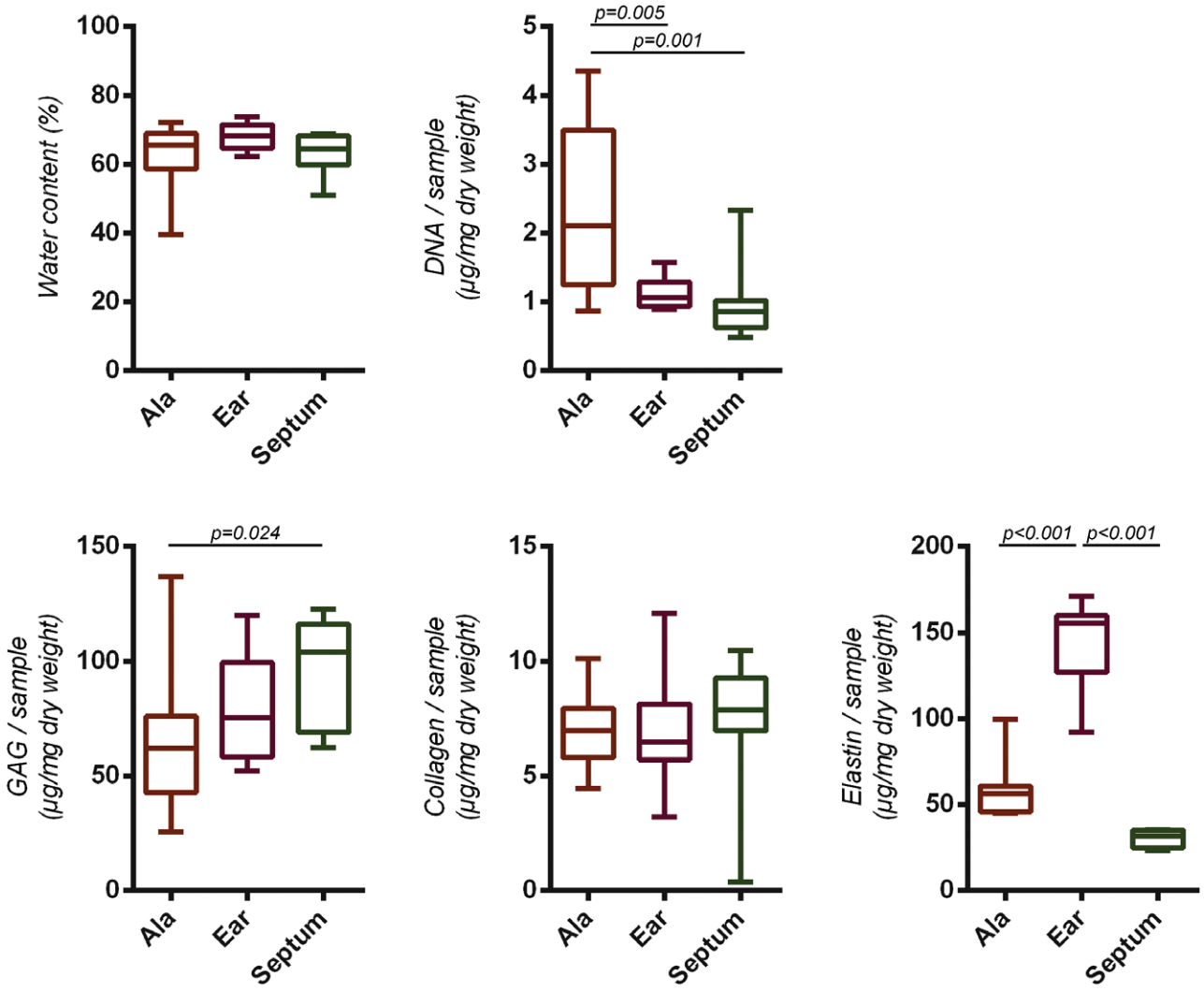

Fig. 3. Biochemical analysis results showing distinct differences in composition between the cartilage types. Although ala nasi cartilage and septum bear strong similarities in tissue architecture, they significantly differ in DNA and GAG content ($P = 0.001$ and $P = 0.024$, respectively). The nasal cartilages contain very limited elastin. This might be partially attributable to connective tissue remnants although caution was taken to remove these as much as possible.

croscopy generated showed a distinct difference between ear cartilage and the cartilage of nasal origin (Fig. 4). Not only the absence of elastin fibers (green) was evident, also the general structure of nasal cartilages was different from the ear. Cartilage from the nasal area gives a much more diffuse image compared with the dense fibrous network of the ear cartilage. Chondrons, agglomerates of chondrocytes within their pericellular matrix, appeared larger in the ala nasi than in the septum in both donors.

DISCUSSION

To our knowledge, this is the first study that compares the biochemical, 3D structural, and mechanical differences between all 3 facial cartilage types in human donors. By measuring differences in cartilage composition, structure, and stiffness on the ECM level, we aimed to identify significant aspects of facial cartilage architecture necessary for adequate tissue engineering.

This is relevant for tissue engineering of cartilage, which has received massive attention the last decade. A variety of different cell types and scaffolds have been proposed for auricular or nasal cartilage engineering.[24–29] Although promising results have been obtained, most regenerated tissues generally are only a very marginal substitution of the original tissue. This study reveals that there are significant differences between cartilage types on the ECM scale, even if they are similar in mechanical properties.

The composition of ear cartilage is known to be different compared with septal cartilage in that it contains elastic fibers.[29] We could measure small amounts of elastin in nasal cartilage with biochemical analyses. This is in line with a study in white New Zealand rabbits where, using immunohistochemical staining, high-elastin content was found specifically in the ear cartilage matrix compared with only moderate elastin content in the nasal septal pericellular regions.[30] The fact that the matrix comprises for an substantial part of elastin suggests that this may offer

Table 1. Bivariate Correlations Model Showing Correlation between Biochemical Composition and Stiffness (Effective Young's modulus) per Cartilage Subtype

Young's Modulus	DNA	GAG	COL	ELA
Auricle				
Pearson	0.040	−0.302	0.080	0.096
Correlation	0.913	0.396	0.826	0.838
Significance (2-tailed)	10	10	10	7
N				
Ala nasi				
Pearson	−0.427	0.327	−0.549	−0.217
Correlation	0.219	0.357	0.100	0.641
Significance (2-tailed)	10	10	10	7
N				
Septum				
Pearson	0.405	0.105	0.408	−0.951*
Correlation	0.246	0.774	0.242	0.049
Significance (2-tailed)	10	10	10	7
N				

Low elastin content has a significant ($P = 0.05$) correlation with the stiffer septum. Question remains whether this is due to the actual elastin concentration or the structural composition.
*Correlation is significant at 0.05 level (2-tailed).

an important attribution to the mechanical qualities of ear cartilage.[31]

The effective Young's modulus was significantly lower in auricular and ala nasi cartilage than in nasal septum cartilage. However, stiffness between ear and ala nasi cartilage was not statistically different, although there was a clear difference in elastin content. These findings match the observations of Griffin et al.[32] who found similar differences in stiffness between ala nasi and septal cartilage.

In a recent article, Nimeskern et al.[33] explored how elastin influences the mechanical behavior of cartilage. They found different viscoelastic behaviors of bovine hyaline articular cartilage and ear cartilage, with ear cartilage being more elastic whereas articular cartilage demonstrated a higher resistance to instantaneous loading. Upon enzymatic treatment to remove elastin and/or GAG, they demonstrated that the compressive mechanical properties of ear cartilage appeared to be mainly due to the elastin fiber network, whereas these properties were provided by collagen in articular cartilage. Moreover, the influence of GAG on mechanical behavior appeared different between the cartilage types: in ear cartilage, GAG had no major influence on mechanics, whereas in articular cartilage, GAG had a clear influence. Although a different tissue, this apparent discrepancy between the expected role of elastin and the actual mechanical properties was also noted in dermal scar tissue.[34] This demonstrates the complex role of tissue composition in mechanical function of the tissue.

The differences in mechanical behavior between the cartilage types could be determined not only by their biochemical compositions but also by tissue architecture. Using multiple-photon laser scanning microscopy, the 3D structure of the different cartilage types could be depicted in high detail. Interestingly, the ala nasi, although very similar in appearance to the septal cartilage and low in elastin content, demonstrated mechanical behavior that is more comparable to ear cartilage. (**See video, Supplemental Digital Content 2**, which displays multiple-photon laser scanning microscopy of the architecture of the ala nasi cartilage in 3D stacked

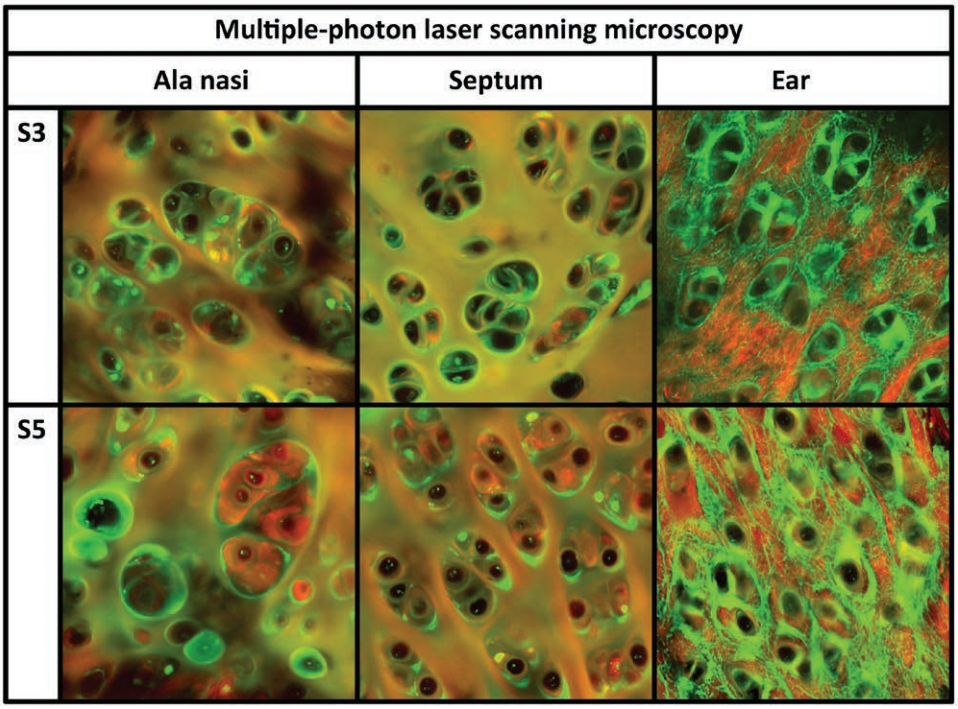

Fig. 4. Top to bottom: donor samples 3 and 5. Left to right: Ala nasi, septum, ear. Green: elastin; red: collagen. The fibrous structures in the ear cartilage are clearly discernable compared with the diffuse green background signal in the nasal cartilage samples. As shown in Figure 3, DNA content varies considerably, which is also discernable in the different cell densities of the septum images.

image video, ***http://links.lww.com/PRSGO/A625*** and **see video, Supplemental Digital Content 3**, which displays multiple-photon laser scanning microscopy of the architecture of the septal cartilage in 3D stacked image video, ***http://links.lww.com/PRSGO/A626***.)

Although similar in general appearance, we observed that chondron size seemed to be different between ala nasi and septum cartilage. Sample size was small however, and no statistic evidence was gathered to support this side finding.

Donor variability is large, and general comparison of our data with literature is difficult as no research has previously been performed comparing these 3 cartilage types both mechanically, structurally, and biochemically. Our data match the observations of Nimeskern et al.[29] that septal cartilage is stiffer and contains higher GAG than auricular cartilage but lower DNA, indicative for lower cell concentration. Our findings also match the results of a study performed by Griffin et al.[32] who measured lower stiffness of the ala nasi cartilage compared with the septum. For tissue engineering purposes, the scale at which the indentation experiments were performed gives a good reference for the appropriate scaffold stiffness on the cellular level. SHG proved a good tool to noninvasively depict the collagen and elastin bundle architecture in 3D. (**See video, Supplemental Digital Content 4**, which displays multiple-photon laser scanning microscopy of the architecture of the ear cartilage in 3D stacked image video, ***http://links.lww.com/PRSGO/A627***.)

This information could be translated to serve as a structural template for 3D printing of scaffolds and together with the data on mechanics and biochemical content provides a new step toward scaffold optimization for facial cartilage reconstruction.

We used cartilage samples from donors at higher age (average 66.5±6 y). Mechanical behavior and histology might differ in younger patients because of calcifications and structural changes during aging. Ears, for example, continue to expand in volume throughout a lifetime, which is attributed to alterations in the elastic fibers during aging.[35] For the septum however, Richmon et al.[16] found no significant differences in mechanical properties between age and gender. Although samples were taken from the same anatomical location in all donors, minor variation might have occurred. This is a limitation, as several studies indicate that within the separate cartilage types, there are regional differences in content.[32] Despite their localization and comparable role as soft-tissue support suggesting similar characteristics, the facial cartilages are in fact quite different from another. The specific function of cartilage tissue, for example, compression for articular cartilage and flexibility for ear cartilage, may demand different mechanical testing regimes. We chose microindentation to explore the stiffness of the ECM; in regard to our findings perhaps a combination of mechanical tests is necessary to be able to elicit the different structural roles of the various cartilage components. In the future, it might be interesting to also include macroscopic mechanical testing, as gross mechanical traits are also influenced by other factors such as the perichondrium and anatomical form.[15,36]

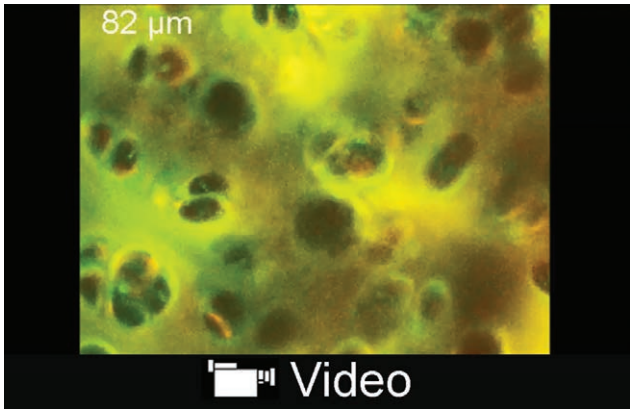

Video Graphic 2. See video, Supplemental Digital Content 3, which displays multiple-photon laser scanning microscopy of the architecture of the septal cartilage in 3D stacked image video. The septal cartilage has a similar appearance to that of the ala nasi with no discernable elastin and aggregated cell clusters throughout the tissue. Step size, 2 µm; green, elastin; red, collagen, ***http://links.lww.com/PRSGO/A626***.

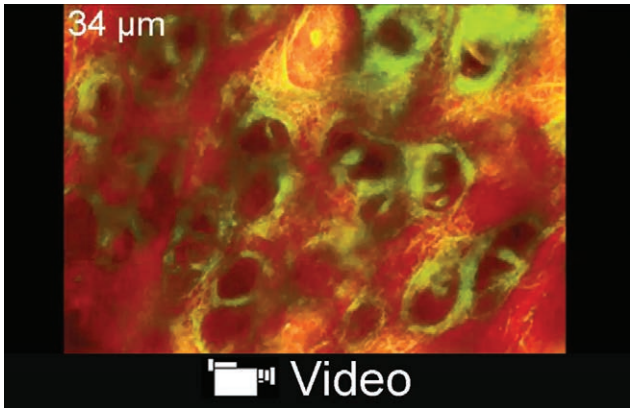

Video Graphic 3. See video, Supplemental Digital Content 4, which displays multiple-photon laser scanning microscopy of the architecture of the ear cartilage in 3D stacked image video. The intricate network of elastin fibers is clearly discernable. Step size, 2 µm; green: elastin; red, collagen, ***http://links.lww.com/PRSGO/A627***.

From a surgical perspective, it is interesting to note that tissue composition and mechanical behavior are not always related as expected. We did not find an explanation for the lower stiffness of ala nasi cartilage. It does support the concept that tissue transplants from different origins can serve as structural surrogate in reconstructive surgery. The use of concha tissue for ala nasi reconstruction is an excellent example thereof. Other fields that are not covered in this article but are important to consider are cellular interaction including proteomics and metabolism, as cell survival and behavior are key to tissue engineering and long-term successful transplantation. The finding that the facial cartilage types not only structurally differ but also vary in cell content may hold implications for surgical reconstruction, as tissues with higher cells concentrations potentially demand a more nutrient-rich environment when transplanted. The merging of knowledge from practical experience and fundamental research in our opinion

will prove essential in a world where tissue engineering is rapidly becoming reality, a development that should not be overlooked by surgeons.

CONCLUSION

Understanding the complete composition of tissue, structural, mechanical, and biochemical, is essential to regenerate an appropriate scaffolding environment for facial cartilage regeneration. This is particularly reflected by the finding that albeit its 3D structural similarity to septal cartilage, the ala nasi has a matrix stiffness that is more comparable to ear cartilage. In that light, the role of elastin remains to be further elicited, and perhaps we should question whether its name is not misleading in regard of its contribution to tissue mechanics.

Paul van Zuijlen, MD, PhD
Burn Center Department
Red Cross Hospital
Vondellaan 13, Beverwijk 1942 LE
The Netherlands
E-mail: p.vanzuijlen@vumc.nl

ACKNOWLEDGMENTS

We wish to thank Professor Bleys MD from the Department of Anatomy UMCU and the staff of the Dr. Tulp Foundation for providing the tissue samples. We further wish to thank Wendy Koevoet, Department of Otorhinolaryngology, Erasmus MC for technical support with biochemical assays and Birgit Witte from the Biostatistics department of the VUMC for statistical support.

REFERENCES

1. Driscoll BP, Baker SR, Drisco BP. Reconstruction of nasal alar defects. *Arch Facial Plast Surg.* 2001;3:91–99.
2. Ray E, Wu T, Nazarian Mobin SS, et al. Review of options for burned ear reconstruction. *J Craniofac Surg.* 2010;21:1165–1169.
3. Kridel RW, Ashoori F, Liu ES, et al. Long-term use and follow-up of irradiated homologous costal cartilage grafts in the nose. *Arch Facial Plast Surg.* 2009;11:378–394.
4. Bhandari PS. Total ear reconstruction in post burn deformity. *Burns* 1998;24:661–670.
5. Yanaga H, Imai K, Fujimoto T, et al. Generating ears from cultured autologous auricular chondrocytes by using two-stage implantation in treatment of microtia. *Plast Reconstr Surg.* 2009;124:817–825.
6. Qing-Hua Y, Yu-Peng S, Haiyue J, et al. The significance of the biomechanical properties of costal cartilage in the timing of ear reconstruction surgery. *J Plast Reconstr Aesthet Surg.* 2011;64:742–746.
7. Anthwal N, Thompson H. The development of the mammalian outer and middle ear. *J Anat.* 2016;228:217–232.
8. Som PM, Naidich TP. Illustrated review of the embryology and development of the facial region, part 1: Early face and lateral nasal cavities. *AJNR Am J Neuroradiol.* 2013;34:2233–2240.
9. Popko M, Bleys RL, De Groot JW, et al. Histological structure of the nasal cartilages and their perichondrial envelope. I. The septal and lobular cartilage. *Rhinology* 2007;45:148–152.
10. Mansfield JC, Winlove CP, Moger J, et al. Collagen fiber arrangement in normal and diseased cartilage studied by polarization sensitive nonlinear microscopy. *J Biomed Opt.* 2008;13:044020.
11. Zhu X, Tang Y, Chen J, et al. Monitoring wound healing of elastic cartilage using multiphoton microscopy. *Osteoarthritis Cartilage* 2013;21:1799–1806.
12. McKee CT, Last JA, Russell P, et al. Indentation versus tensile measurements of Young's modulus for soft biological tissues. *Tissue Eng Part B Rev.* 2011;17:155–164.
13. Britt JC, Park SS. Autogenous tissue-engineered cartilage: evaluation as an implant material. *Arch Otolaryngol Head Neck Surg.* 1998;124:671–677.
14. Reiffel AJ, Kafka C, Hernandez KA, et al. High-fidelity tissue engineering of patient-specific auricles for reconstruction of pediatric microtia and other auricular deformities. *PLoS One* 2013;8:e56506.
15. Westreich RW, Courtland HW, Nasser P, et al. Defining nasal cartilage elasticity: biomechanical testing of the tripod theory based on a cantilevered model. *Arch Facial Plast Surg.* 2007;9:264–270.
16. Richmon JD, Sage AB, Wong VW, et al. Tensile biomechanical properties of human nasal septal cartilage. *Am J Rhinol.* 2005;19:617–622.
17. Hsieh CH, Lin YH, Lin S, et al. Surface ultrastructure and mechanical property of human chondrocyte revealed by atomic force microscopy. *Osteoarthritis Cartilage* 2008;16:480–488.
18. Sanchez-Adams J, Wilusz RE, Guilak F. Atomic force microscopy reveals regional variations in the micromechanical properties of the pericellular and extracellular matrices of the meniscus. *J Orthop Res.* 2013;31:1218–1225.
19. Marrese M, Guarino V, Ambrosio L. Atomic force microscopy: a powerful tool to address scaffold design in tissue engineering. *J Funct Biomater.* 2017;8:E7.
20. Guilak F, Cohen DM, Estes BT, et al. Control of stem cell fate by physical interactions with the extracellular matrix. *Cell Stem Cell* 2009;5:17–26.
21. Little CJ, Bawolin NK, Chen X. Mechanical properties of natural cartilage and tissue-engineered constructs. *Tissue Eng Part B Rev.* 2011;17:213–227.
22. Chavan D, van de Watering TC, Gruca G, et al. Ferrule-top nanoindenter: an optomechanical fiber sensor for nanoindentation. *Rev Sci Instrum.* 2012;83:115110.
23. Oliver WC, Pharr GM. An improved technique for determining hardness and elastic modulus using load and displacement sensing indentation experiments. *J Mater Res.* 1992;7:1564–1583.
24. Tay AG, Farhadi J, Suetterlin R, et al. Cell yield, proliferation, and postexpansion differentiation capacity of human ear, nasal, and rib chondrocytes. *Tissue Eng.* 2004;10:762–770.
25. Kobayashi S, Takebe T, Inui M, et al. Reconstruction of human elastic cartilage by a CD44+ CD90+ stem cell in the ear perichondrium. *Proc Natl Acad Sci U S A.* 2011;108:14479–14484.
26. Kusuhara H, Isogai N, Enjo M, et al. Tissue engineering a model for the human ear: assessment of size, shape, morphology, and gene expression following seeding of different chondrocytes. *Wound Repair Regen.* 2009;17:136–146.
27. Yanaga H, Yanaga K, Imai K, et al. Clinical application of cultured autologous human auricular chondrocytes with autologous serum for craniofacial or nasal augmentation and repair. *Plast Reconstr Surg.* 2006;117:2019–2030; discussion 2031.
28. Hellingman CA, Verwiel ET, Slagt I, et al. Differences in cartilage-forming capacity of expanded human chondrocytes from ear and nose and their gene expression profiles. *Cell Transplant.* 2011;20:925–940.
29. Nimeskern L, Pleumeekers MM, Pawson DJ, et al. Mechanical and biochemical mapping of human auricular cartilage for reliable assessment of tissue-engineered constructs. *J Biomech.* 2015;48:1721–1729.
30. Naumann A, Dennis JE, Awadallah A, et al. Immunochemical and mechanical characterization of cartilage subtypes in rabbit. *J Histochem Cytochem.* 2002;50:1049–1058.
31. Nimeskern L, van Osch GJ, Müller R, et al. Quantitative evaluation of mechanical properties in tissue-engineered auricular cartilage. *Tissue Eng Part B Rev.* 2014;20:17–27.

32. Griffin MF, Premakumar Y, Seifalian AM, et al. Biomechanical characterisation of the human nasal cartilages; implications for tissue engineering. *J Mater Sci Mater Med.* 2016;27:11.
33. Nimeskern L, Utomo L, Lehtoviita I, et al. Tissue composition regulates distinct viscoelastic responses in auricular and articular cartilage. *J Biomech.* 2016;49:344–352.
34. Verhaegen PD, Schouten HJ, Tigchelaar-Gutter W, et al. Adaptation of the dermal collagen structure of human skin and scar tissue in response to stretch: an experimental study. *Wound Repair Regen.* 2012;20:658–666.
35. Ito I, Imada M, Ikeda M, et al. A morphological study of age changes in adult human auricular cartilage with special emphasis on elastic fibers. *Laryngoscope* 2001;111:881–886.
36. Roy R, Kohles SS, Zaporojan V, et al. Analysis of bending behavior of native and engineered auricular and costal cartilage. *J Biomed Mater Res A* 2004;68:597–602.